# Обзор ArXiv/astro-ph, 1-8 июня 2022

От Сильченко О.К.

# ArXiv: 2206.01578

# Dorado and its member galaxies. III

## Mapping star formation with FUV imaging from UVIT. ⋆

R. Rampazzo[1,2], P. Mazzei[2], A. Marino[2], L. Bianchi[3], J. Postma[4],
R. Ragusa[5], M. Spavone[5], E. Iodice[5], S. Ciroi[6], and E.V. Held[2]

[1] INAF-Osservatorio Astrofisico di Asiago,Via dell'Osservatorio 8, 36012 Asiago, Italy e-mail: roberto.rampazzo@inaf.it
[2] INAF-Osservatorio Astronomico di Padova, Vicolo dell'Osservatorio 5, 35122 Padova, Italy
[3] Dept. of Physics & Astronomy, The Johns Hopkins University, 3400 N. Charles St., Baltimore, MD 21218, USA
[4] University of Calgary, 2500 University Drive NW, Calgary, Alberta, Canada
[5] INAF-Osservatorio Astronomico di Capodimonte, Salita Moiariello 16, 80131 Napoli, Italy
[6] Department of Physics and Astronomy "G. Galilei", University of Padova, Vicolo dell'Osservatorio 3, 35122 Padova, Italy

April 6, 2022 ; May 30, 2022

**ABSTRACT**

*Context.* We are investigating the star formation in galaxies of the actively evolving Dorado group where, for a large fraction of both early- and late-type galaxies, signatures of interactions and merging events are revealed by optical and radio observations.
*Aims.* Our previous H$\alpha$+[N II] study, probing ≈10 Myrs timescales, suggested that star formation is still ongoing in early-type galaxies. In this work, we use far-UV (FUV) imaging to map recent star formation on longer times scales, of the order of 100 Myrs.
*Methods.* We used the Ultraviolet telescope UVIT on board Astrosat to image the galaxies of the Dorado backbone previously observed in H$\alpha$+[N II] , with the far-UV filter FUV.CaF2 (1300-1800 Å). The sample includes NGC 1536, NGC 1546, NGC 1549, [CMI2001]4136-01, NGC 1553, IC 2058, PGC 75125,NGC 1566, NGC 1596 and NGC 1602; for the two latter galaxies, the UVIT data provide the first view in far-UV. For the others, previously observed by GALEX, the UVIT data afford a ∼ 5× improvement in spatial resolution.
*Results.* FUV.CaF2 emission is revealed in all the Dorado galaxies observed, tracing young stellar populations in ring structures and showing tidal distortions. The Sérsic index, derived by fitting the luminosity profiles, is always $n < 3$ suggesting that the FUV.CaF2 emission originates from a disk also in early-type galaxies. The star formation rate (SFR) ranges from 0.004±0.001 $M_\odot yr^{-1}$ of [CMI2001]4136-01 to 2.455±0.027 $M_\odot yr^{-1}$ of NGC 1566. Most of the recent star formation is found at the periphery of the Dorado group where most of late-type galaxies are located. For these galaxies, the ratio $SFR_{H\alpha}/SFR_{FUV.CaF2}$ is close to 1, except for the edge-on IC 2058, similarly to previously reported relations for Local Volume samples. For early-type galaxies, however, $SFR_{H\alpha}$ is about 15 times higher than $SFR_{FUV}$. The Dorado's early-type galaxies define a separate locus in $SFR_{FUV}$, $SFR_{H\alpha}$ space with respect to the late-type galaxies, which is well represented by the relation $\log(SFR_{FUV.CaF2}) = 0.70 \times \log(SFR_{H\alpha}) - 1.26$.
*Conclusions.* The disk structure of the FUV.CaF2 emitting populations discovered in all the early-types galaxies implies dissipative processes and wet merging events. The systematic discrepancy between SFRs derived from H$\alpha$ and FUV fluxes suggests that rejuvenation episodes in early-type galaxies cannot sustain constant star formation over ∼100 Myrs timescales.

# Группа Dorado

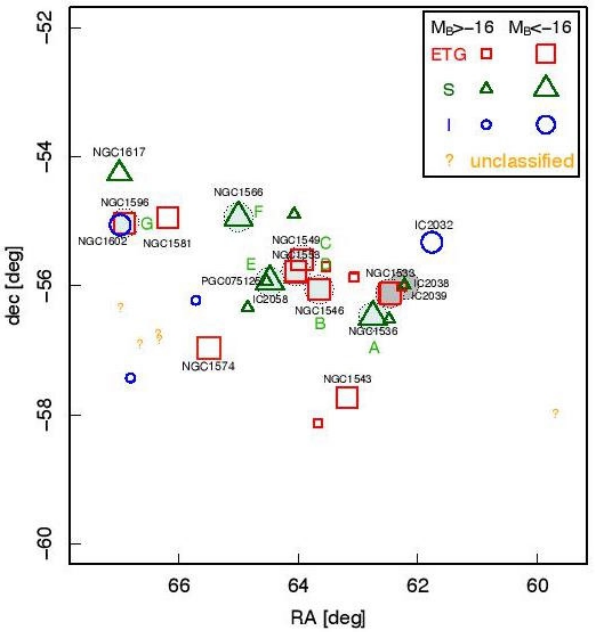


**Fig. 1.** Projected distribution of Dorado galaxy members according to Firth et al. (2006) and Kourkchi & Tully (2017). Members are labelled according to their morphology and B-Band magnitude provided by HyperLeda. UVIT FUV.CaF2 fields listed in Table 1, are enclosed by a light-green circle having the diameter of the UVIT field (28′). Target galaxies within each field are also labelled. The morphological, photometric and star forming properties obtained from the UVIT FUV.CaF2 data-set about NGC 1533, IC 2038/2039, dark-grey circles in the figure, have been presented and discussed in in Ram2021. Ram2020 also observed NGC 1581 and NGC 1543 in H$\alpha$+[N II] . All galaxies but the NGC 1596/NGC 1602 have been already observed with GALEX at lower resolution and sensitivity (see e.g. Marino et al. 2011a,b).

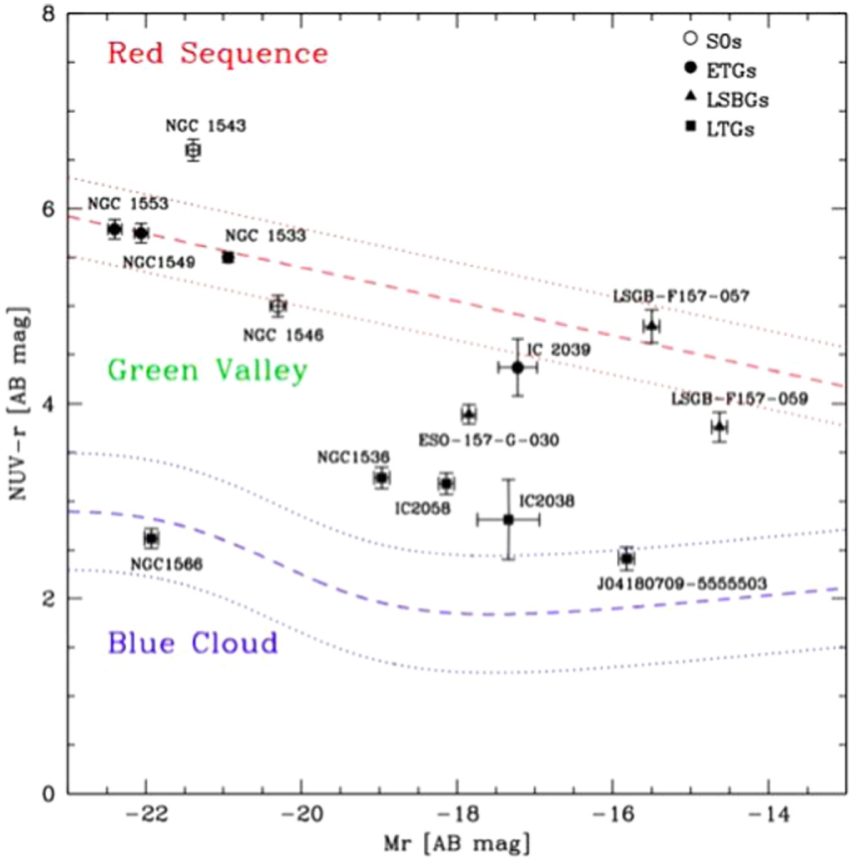

# Ram pressure? NGC 1566, GALEX

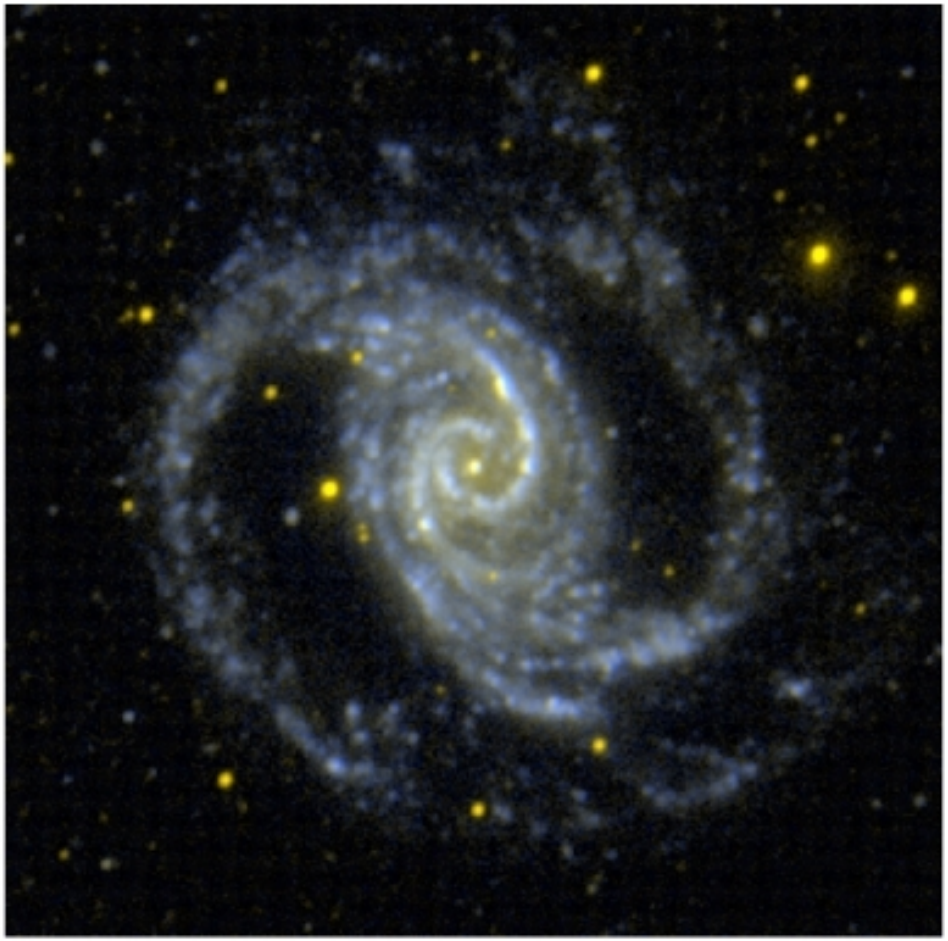

# Наблюдения на индийском ультрафиолетовом телескопе

### 3. Observations and data reduction

Astrosat is a X-ray - UV observatory launched by the Indian Space Research Organization on September 28, 2015. The Ultra-Violet Imaging Telescope facility UVIT (Tandon et al. 2017) is composed of two Ritchey-Chretien telescopes with 37.5 cm aperture, a circular field of view of 28′ diameter, originally observing simultaneously one in FUV (1300-1800 Å) and the other both in Near UV (NUV) (2000-3000 Å) and optical band, VIS (3200-5500 Å), by means of a beam-splitter directing NUV and VIS to individual cameras.

The NUV detector is currently not working. Therefore, observations have been performed with the FUV channel only. We used the full field of view, in photon counting mode, with the Filter F148W CaF2 ($\lambda_{mean}$=1481, $\Delta\lambda$=500Å). Photons are counted

# Выборка: от центральной cD до карликов поздних типов

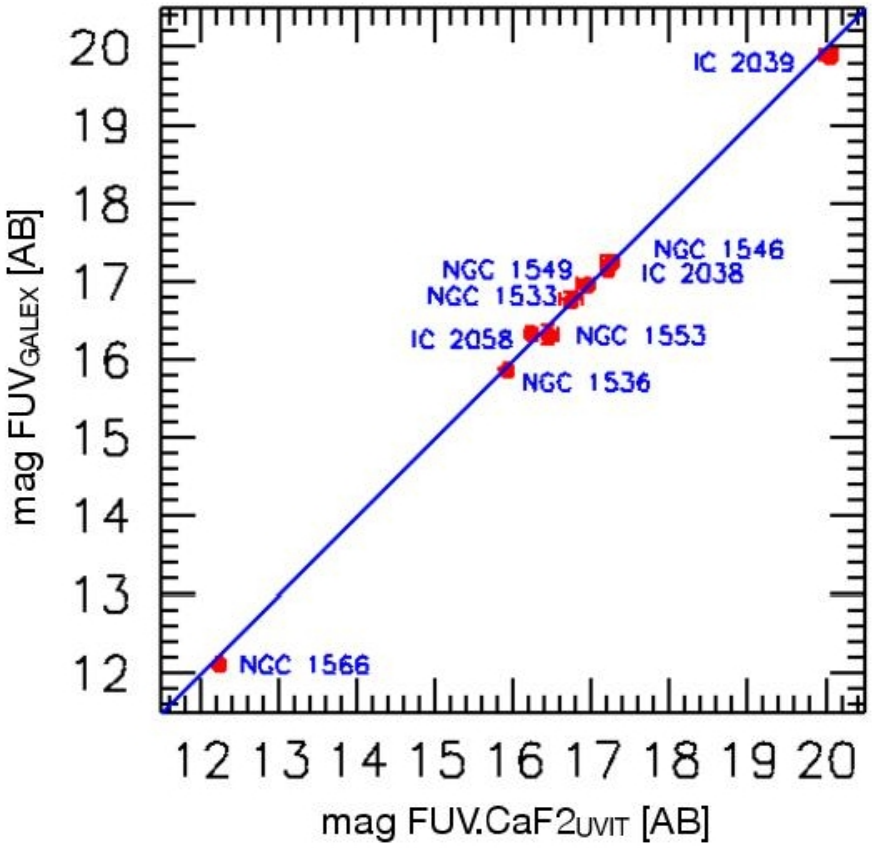


**Fig. 2.** Comparison with FUV GALEX magnitudes reported in Table 1. The comparison includes galaxies in Ram2021, namely NGC 1533, IC 2038 and IC 2039, whose magnitudes are corrected for foreground Galactic extinction as described in their Table 3.

FUV

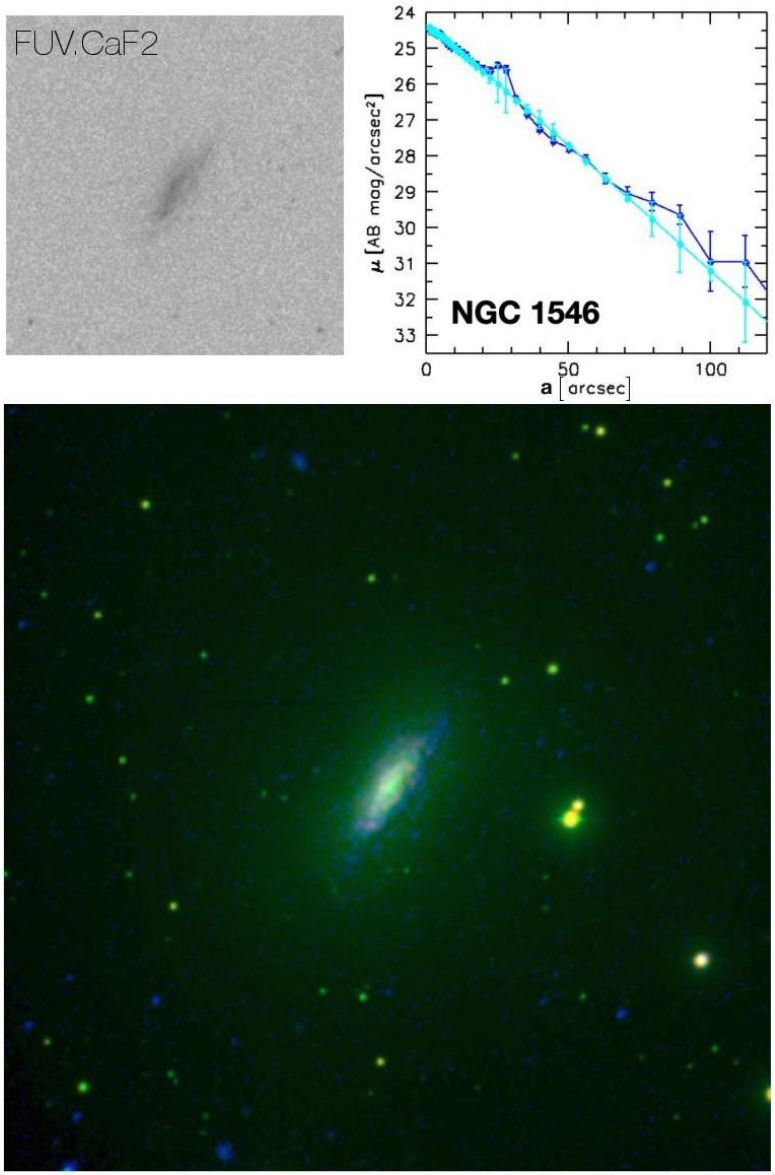


Composite: g, H-alpha+[NII],…

**Fig. 5.** As in Figure 4 for NGC 1546. The image size is 7′×7′. North is on the top and East to the left.

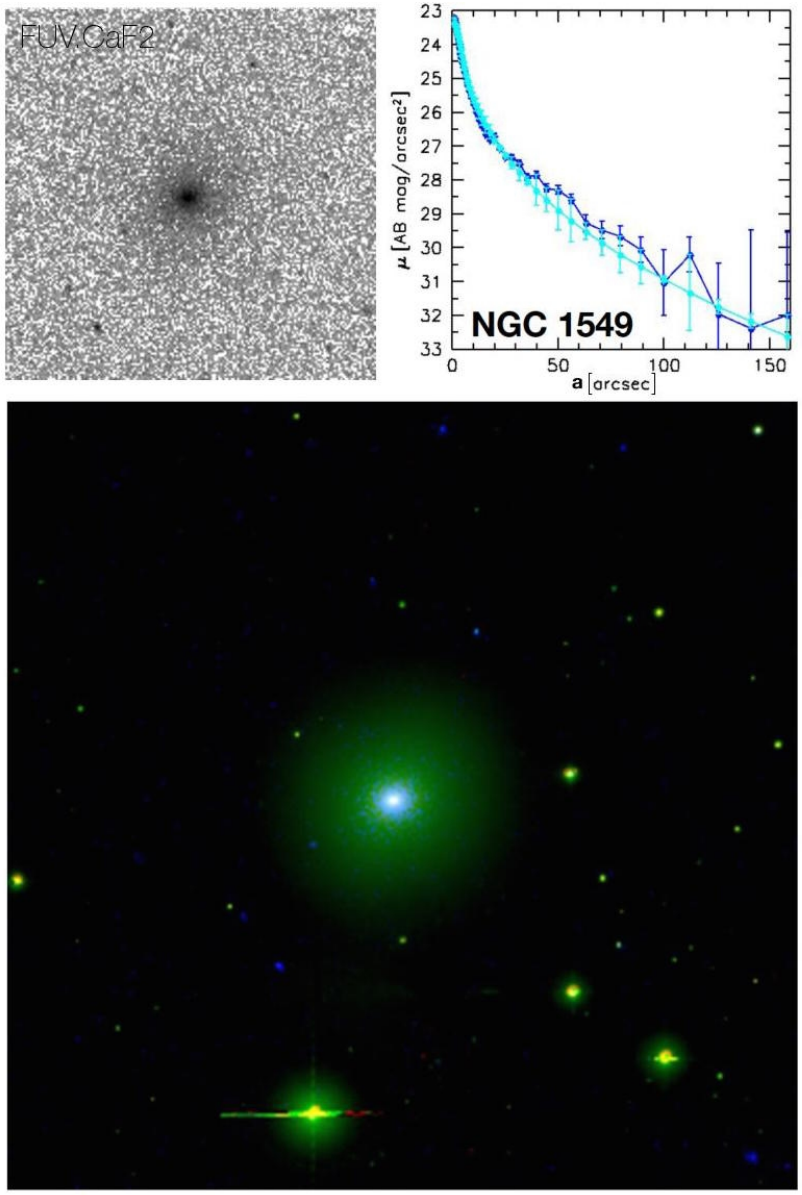


**Fig. 6.** As in Figure 4 for NGC 1549. The image size is 8′×8′. North is on the top and East to the left.

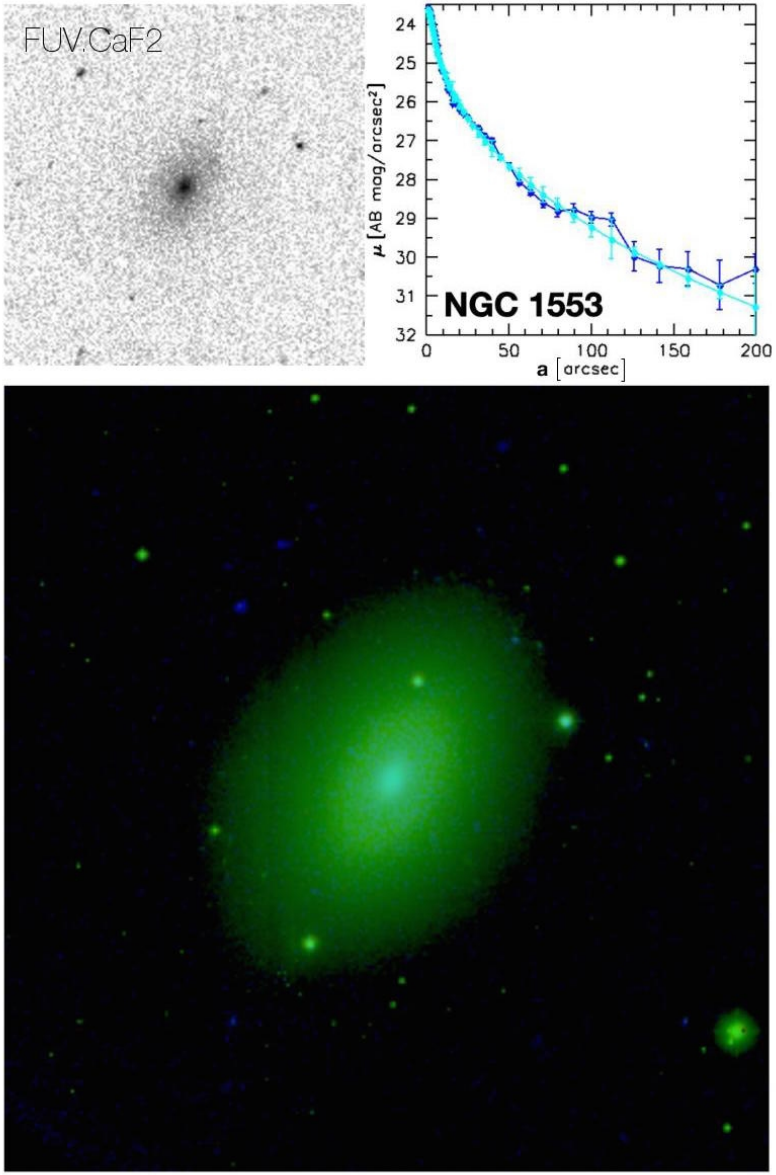


**Fig. 7.** As in Figure 4 for NGC 1553. The image size is 7′×7′. North is on the top and East to the left.

# А вот поздние типы…

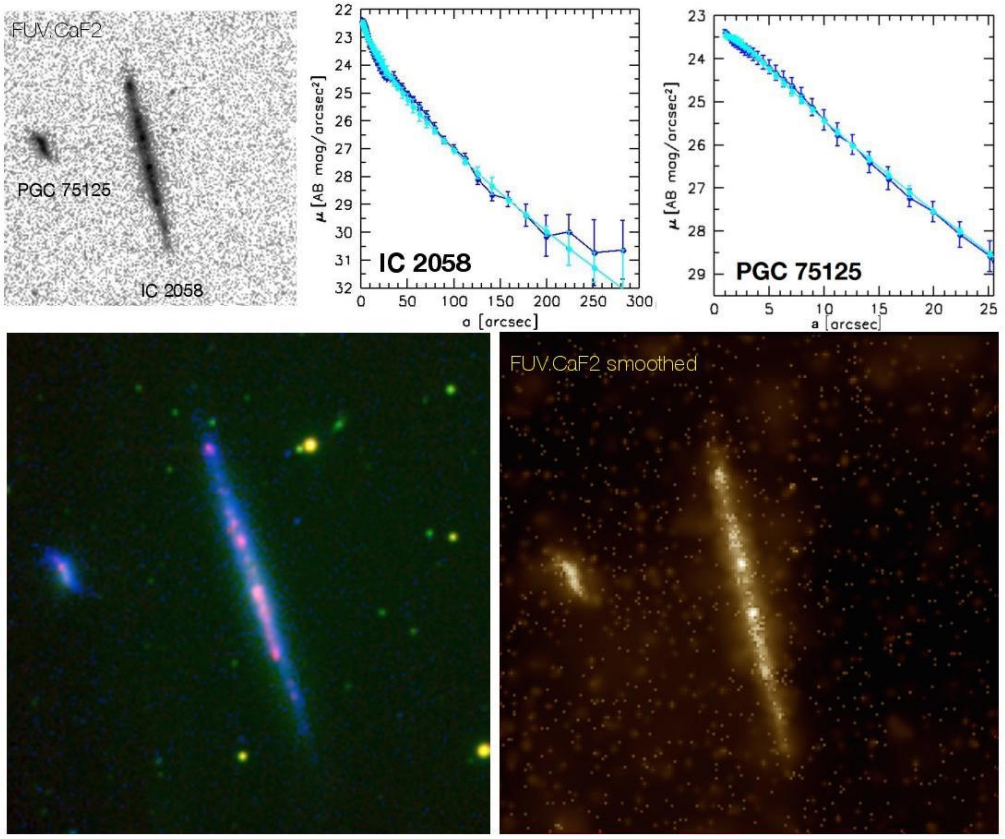


**Fig. 9.** (*Top left panel)* UVIT FUV.CaF2 image of IC 2058 and PGC 75125 at the centre of the frame and at the East side, respectively. The image size is 5′×5′. North is on the top and East to the left. *(Top central panel)* FUV.CaF2 surface brightness profile (blue) of IC 2058 and *(top right panel)* of PGC 75125. Single Sérsic law is superposed (cyan), to fit the light profile. (*Bottom left panel*) Colour-composite RGB image of IC 2058 and PGC 75125 as in Figure 4. (*Bottom right panel*) FUV.CaF2 image smoothed using the AMOOTH task with $\tau_{min}$=1.5.

# NGC 1596: Полярный диск?

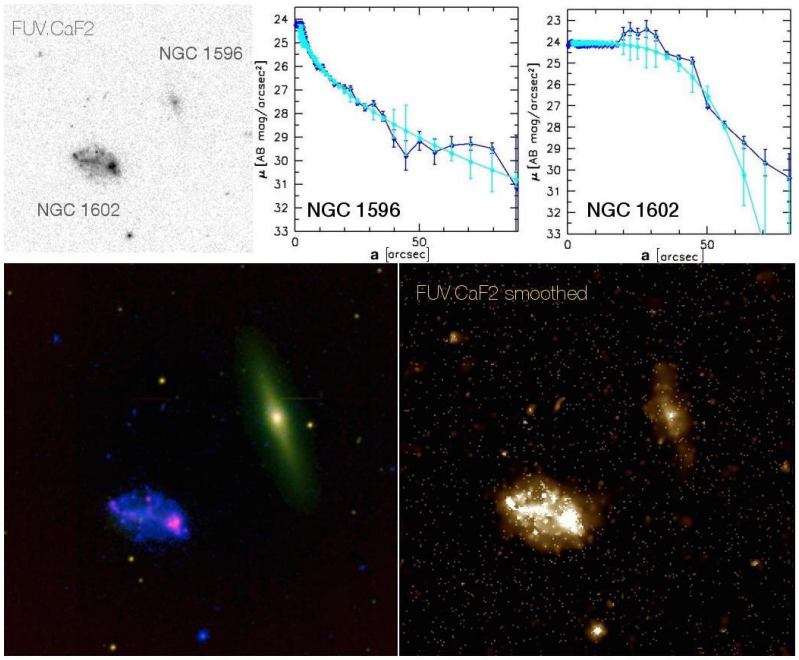


**Fig. 11.** (*Top left panel)* UVIT FUV.CaF2 image of NGC 1596 (North-west ) and NGC 1602 (South-East). The image size is 7′×7′. North is on the top and East to the left. (*Top right panels*) FUV.CaF2 surface brightness profiles of NGC 1596 and NGC 1602 (blue solid lines). The fit of a single Sérsic law is overlaid to the luminosity profile (cyan squares). *(Bottom left panel)* Colour composite RGB image of NGC 1596 and NGC 1602 as in Figure 4.(*Bottom right panel*) FUV.CaF2 image smoothed using ASMOOTH task, with $\tau_{min}$=1.5.

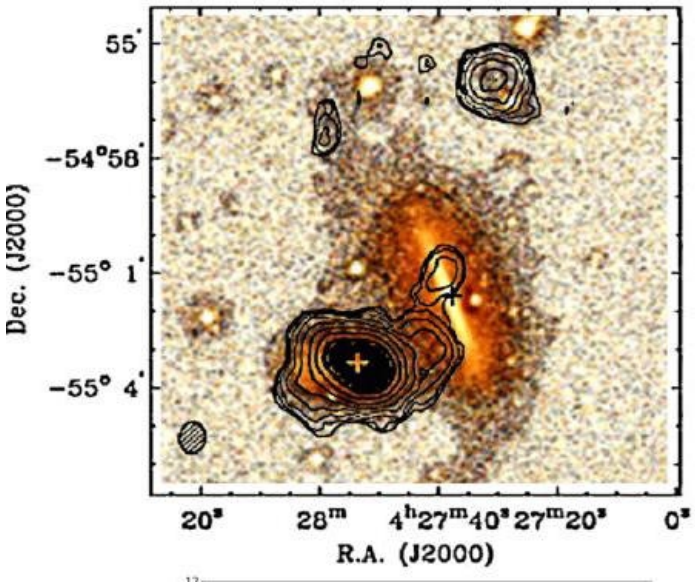

# Результаты по звездообразованию

**Table 3.** Integrated magnitudes of Dorado in UVIT FUV.CaF2.

| **Field** | **ID source** | **FUV.CaF2 AB [mag]** | $\langle\epsilon\rangle$ | $\langle PA\rangle$ **[deg]** | n | $L_{FUV.CaF2}$ **$10^{26}$ [erg s$^{-1}$ Hz$^{-1}$]** | SFR **[$M_\odot$ yr$^{-1}$]** |
|---|---|---|---|---|---|---|---|
| A | **NGC 1536** | 15.90±0.02 | 0.40 | 160 | 0.76±0.02 | 5.95±0.05 | 0.083±0.001 |
| B | **NGC 1546** | 17.24±0.11 | 0.66 | 141 | 0.98±0.04 | 1.74±0.08 | 0.024±0.001 |
| C | **NGC1549** | 16.92±0.11 | 0.07 | 0 | 2.86±0.28 | 2.32±0.01 | 0.033±0.001 |
| | [CMI2001]4136-01 | 19.13±0.34 | ... | ... | ... | 0.30±0.04 | 0.004±0.001 |
| D | **NGC 1553** | 16.44±0.13 | 0.36 | 150 | 2.67±0.21 | 3.63±0.20 | 0.051±0.003 |
| E | **IC 2058** | 16.22±0.04 | 0.74 | 18 | 1.48±0.10 | 4.43±0.07 | 0.062±0.001 |
| | **PGC 075125** | 18.07±0.10 | 0.36 | 20 | 1.20±0.03 | 0.81±0.03 | 0.011±0.0005 |
| F | **NGC 1566** | 12.13±0.03 | 0.05 | 15 | 0.94±0.05 | 175.30±1.93 | 2.455±0.027 |
| G | **NGC 1596** | 17.96±0.21 | 0.52 | 20 | 2.12±0.18 | 0.95±0.08 | 0.013±0.001 |
| | **NGC 1602** | 15.06±0.04 | 0.32 | 80 | 0.25±0.04 | 12.94±0.21 | 0.181±0.003 |

**Notes.** Col. 2 gives the galaxy identification; Col. 3 gives the extinction corrected FUV integrated magnitude; Col. 4 gives the average ellipticity; Col. 5 gives the average Position Angle; Col. 6 gives the Sersíc index; Col. 7 gives the total absolute FUV luminosity; col. 8. gives the SFR as derived from eq.1.

# По H-alpha SFR больше…

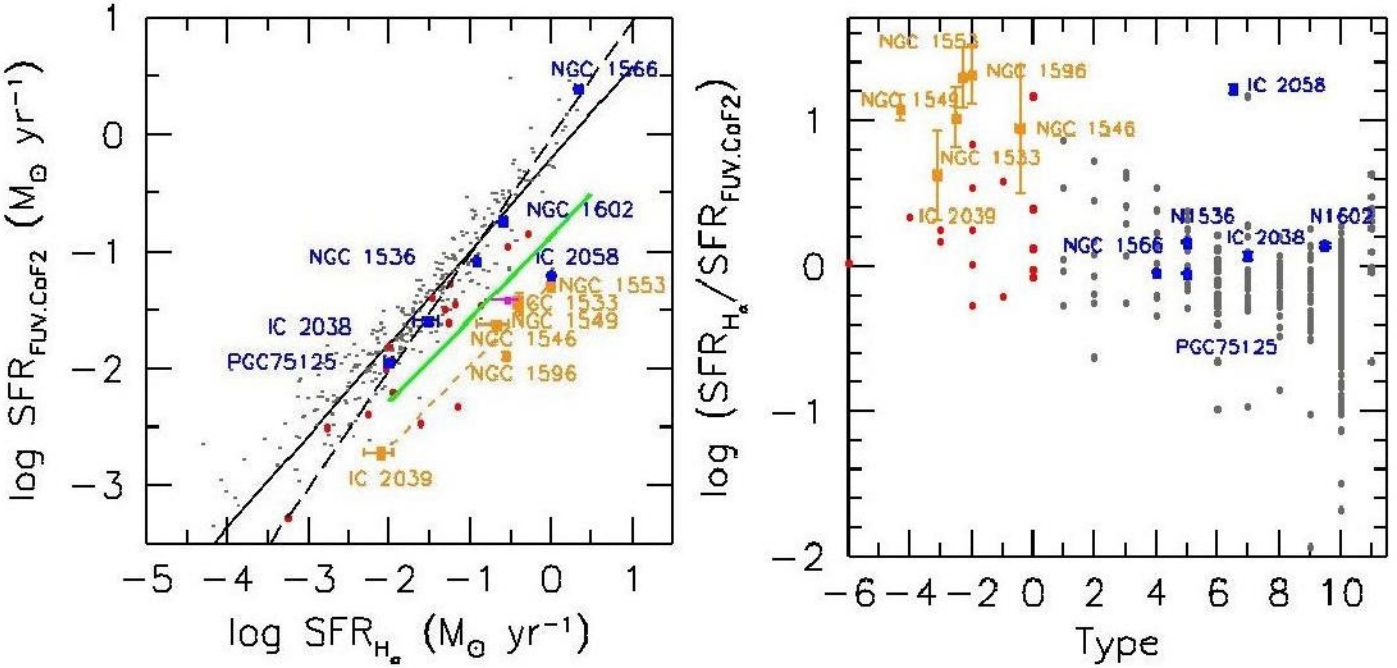


**Fig. 15.** *(Left panel):* Comparison between SFR derived from H$\alpha$ and FUV.CaF2 luminosities. The Dorado sample is plotted with orange (ETG) and blue (LTG) squares. For comparison, we plot Lee et al. (2009, their Table 2) sample with red (ETG) and gray (LTG) dots. The magenta dot shows NGC1533 as derived using SFR from H$\alpha$ by Kaisina et al. (2012) and from FUV.CaF2 measured in this work. All measures account for Galactic extinction, but internal dust attenuation has not been modelled and accounted for. The black solid and dashed lines show the Lee et al. (2009) relation and the one-to-one correspondence, respectively. The solid green and orange-dashed lines are the regression fit of the entire Dorado sample (equation 3) and of the ETGs members (equation 2), respectively. *(Right panel):* Ratio of SFR from H$\alpha$ and FUV.CaF2 versus galaxy morphological type.

# Короткая шкала? Или азот?

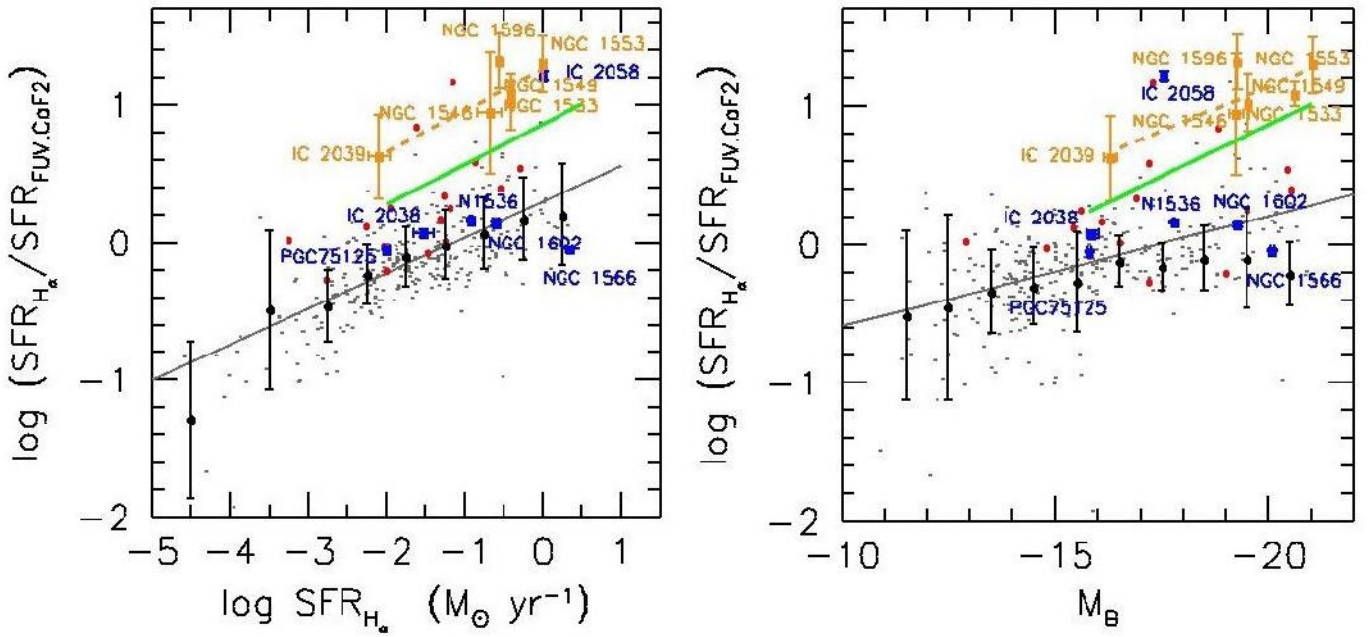


**Fig. 16.** Ratio between the SFR from H$\alpha$ and FUV.CaF2 luminosities in logarithmic scale versus the SFR from H$\alpha$ (left panel) and the absolute B-band magnitude (right panel). Symbols used are the same as in Figure 15. Black dots are average values of the sample of Lee et al. (2009, their Table 2). Solid grey lines are the linear least squares fits by Lee et al. (2009). The solid green and orange dashed dashed lines are the regression fit of the entire Dorado sample (equation 4 in left panel and equation 6 in the right panel) and for the ETGs (equation 5 in left panel and equation 7 in the right panel), respectively.